

## THEORETICAL TREATMENT FOR THE TIME DEPENDENT EXTERNAL FIELD EFFECT ON THE SPIN CHANNELS OF T-SHAPED DOUBLE QUANTUM DOTS COUPLED TO (HALF-METALLIC SCsN BULK) LEADS

Maged A. nattiq<sup>a</sup>, Jenan M. Al-Mukh<sup>a</sup>, Jabber M. Khalaf Al-Zyadi<sup>a</sup>

<sup>a</sup> Department of Physics, College of Education for Pure Sciences, University of Basrah, Iraq

### ABSTRACT

The external time dependent field-assisted spin transport through T-shaped double quantum dots embedded between two ferromagnetic leads are studied and analyzed. The time – dependent Hamiltonian, that describes the device, follows the tight binding scheme in taking all the spin dependent coupling interactions between the subsystems into consideration. The theoretical treatment is accomplished using the time – evolution operator approach, since the equations of motion in the interaction representation for the time – evolution operator matrix elements are derived. The thirty two integro-differential equations of motion for both spin are solved numerically. The energy dependent calculations are achieved by considering the density of states of the ferromagnetic leads. While the adiabatic approximation is used to treat the effects of the external time dependent field characteristics (frequency and amplitude ) theoretically. In concern to the ferromagnetic leads, the study utilizes the first-principles full-potential linearized augmented plane-wave method (FP-LAPW), this method depends on the use of the density functional theory to examine the structural, magnetic, and electronic characteristics of the bulk of ZB ScSn. This study has proven that the bulk ZB ScSn is half- metallic ferromagnet at an equilibrium lattice constant of (0.6697 nm). The main goal of our study is to investigate the effects of the external time dependent field on the T-shaped double quantum dots device, so all the electronic properties of the device are taken into consideration in our treatment. The role of the field frequency and the spin dependent coupling interaction are well analyzed and explained for the ScSn bulk leads.

**Keywords:** spintronics, half metallic density of states, time – dependent spin transport, time-evolution operator technique.

### 1 - Introduction

The most studied systems both theoretically and experimentally, that display very rich physics, are single, double, and triple-quantum dot systems. At nano scale length, many new, meaningful and unique physical properties, such as quantum interferences [1-5], Fano effect [6–8], Kondo effect [9,10], thermoelectric effect [11,12] and photon assisted tunneling effect [13,14] were found and investigated in the quantum dot systems. These novel features have been exploited in optoelectronics and quantum computing [15]. DQDs offer ideal play area to observe various correlations at the nanoscale. Since the behavior of such systems simulates the behavior of real molecules. In comparison with a single QD structure, the double coupled quantum-dot systems provide more channels [16] for the electron transmission and possess more controlled parameters to fabricate the electronic transport properties [17–22]. In serial and parallel DQD structures, experiments established that an extraordinary control over the physical properties of DQDs via the

interdot hopping can be achieved [21,22]. The important aim of quantum technologies is to employ entangled states in isolated, well-defined systems in a tunable manner. Decoherence, which challenges the correlation between entangled parties through the coupling with the environment, is a main opponent of those quantum technologies, including quantum computation. In the T-shaped DQDs, only one central quantum dot connects to two leads via coupling tunneling interaction, while the other one is side coupled to the central one. Usually, a single energy level is included on each dot. In such configurations, there exist two channels giving rise to quantum interference; one is through the central quantum dot and the other is through the side quantum dot [23,24].

Recently, the time dependent quantum transport merit of quantum dot systems has considered a vital research area consequent for potential applications in nano-electronic devices. Application of external *ac* field on a quantum dot system leads to the time dependent quantum transport and one of the essential features is the well-known photon assisted tunneling.

Our study aims to analyze and investigate the time – dependence of spin transport through T-shaped double quantum dots, coupled to ferromagnetic leads, in presence of external time dependent field. To achieve our aim, the time evolution of the T-shaped double quantum dots charge and spin currents flowing in the system are described in terms of the time – evolution operator which is given by the equation of motion in the interaction representation. This extended theoretical treatment, which takes all the quantum interference effects into consideration, is invested to write program by Fortran language to calculate the time and spin dependence of the transport properties of the device. In concern to the leads, the first-principles full-potential linearized augmented plane-wave method (FP-LAPW), that depends on using of the density functional theory is used to examine the structural, magnetic, and electronic characteristics of the bulk ZB ScSn. Since, thin structure can be used as leads for the device considered in our study.

## **2 - Model Calculation**

In this study, we consider T- shaped double quantum dots (see fig.(1)). The quantum dot QD1 is embedded between two ferromagnetic leads while the second quantum dot QD2 is side coupled to the first one. Two different density of states biased structures in each lead may break the symmetry of the system. From experimental point of view such study is important because in real nano-systems, the leads are often characterized by nontrivial band structures i.e. band with peaks, surface states or gapes. So the lead's density of states plays a crucial role in the spin transport in nano-systems.

The time evolution operator method [25] which was successfully applied for time dependent of the external perturbations is used in our treatment. In the study we take the following into consideration :

- 1- The presence of external time dependent field applied to subsystems including the time dependent of the quantum dots energy levels.
- 2- The time and spin dependent transport through the spin dependent tunneling barriers with ferromagnetic leads.
- 3- The equations of motion that must be solved are for both spin, neglecting the correlation effects.

- 4- The direct coupling interaction between the quantum dots is considered as a spin dependent one.
- 5- The spin dependent Fermi distribution function for the electrons in the ferromagnetic leads.

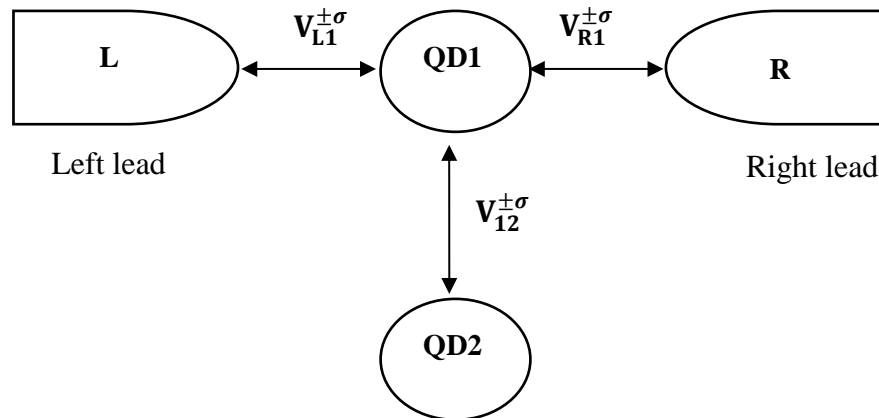


**Fig. (1): Schematic illustration for the double quantum dots forming a T- shaped configuration between two leads.**

### 2-1 The Model Hamiltonian

In order to describe the system considered in our study, we use the following Hamiltonian is used [26]:

$$H(t) = H_0 + V(t) \quad (1)$$

$$H_0 = H_R + H_L + H_{D1} + H_{D2} \quad (2)$$

$$H_R = \sum_{k_R, \sigma} E_{k_R}^{\sigma} n_{k_R}^{\sigma}$$

$$H_L = \sum_{k_L, \sigma} E_{k_L}^{\sigma} n_{k_L}^{\sigma}$$

$$H_{D1} = \sum_{\sigma} E_1^{\sigma} n_1^{\sigma}$$

$$H_{D2} = \sum_{\sigma} E_2^{\sigma} n_2^{\sigma} \quad (3)$$

Where,  $H_{\alpha}$  ( $\alpha = L, R$ ) describe the right and left leads and  $H_{Di}$  ( $i = 1, 2$ ) model the double quantum dots.  $E_{k_{\alpha}}^{\sigma}$  denotes the energy levels of the leads and  $E_i^{\sigma}$  denote the energy levels of the quantum dots for certain spin  $\sigma$ . The occupation numbers  $n_{k_{\alpha}}^{\sigma}$  and  $n_i^{\sigma}$  are given by :

$$\begin{aligned} n_{k_\alpha}^\sigma &= C_{k_\alpha}^{\sigma\dagger} C_{k_\alpha}^\sigma \\ n_i^\sigma &= C_i^{\sigma\dagger} C_i^\sigma \end{aligned} \quad (4)$$

Where  $C_i^{\sigma\dagger}$  ( $C_i^\sigma$ ) is the creation (annihilation) operator of the electrons with spin  $\sigma$  in the dot.  $C_{k_\alpha}^{\sigma\dagger}$  ( $C_{k_\alpha}^\sigma$ ) is the creation (annihilation) operator of the electron with energy  $E_{k_\alpha}^\sigma$  and spin  $\sigma$  in the lead  $\alpha$ . The tunneling Hamiltonian can be given by,

$$\begin{aligned} V^\sigma(t) &= V_{12}^\sigma(t) C_1^{\sigma\dagger}(t) C_2^\sigma(t) + V_{21}^\sigma(t) C_2^{\sigma\dagger}(t) C_1^\sigma(t) \\ &+ \sum_\alpha \sum_{k_\alpha} [V_{1k_\alpha}^\sigma(t) C_1^{\sigma\dagger}(t) C_{k_\alpha}^\sigma(t) + V_{k_\alpha 1}^\sigma(t) C_{k_\alpha}^{\sigma\dagger}(t) C_1^\sigma(t)] \end{aligned} \quad (5)$$

The tunneling coupling matrix elements between the central quantum dot and the leads are denoted by  $V_{1k_\alpha}^\sigma$ . While  $V_{12}^\sigma$  denotes the coupling interaction between the central quantum dot and the side coupled one.

### 2-2 The Equations of Motion Formulation

The time evolution of the T-shaped DQD charge and current flowing in the system can be described in terms of the time- evolution operator  $U(t, t_0)$  given by the equation of motion in the interaction representation (in atomic unit) [27-31],

$$i \frac{\partial U(t, t_0)}{\partial t} = \tilde{V}^\sigma(t) U(t, t_0) \quad (6)$$

where,

$$\tilde{V}^\sigma(t) = U_0(t, t_0) V^\sigma(t) U_0^\dagger(t, t_0) \quad (7)$$

It is assumed that the interaction between the subsystems are switched on the distant past  $t_0$ , and,  $U_0(t, t_0) = e^{iH_0(t-t_0)}$  (8)

Here  $H_0$  denotes the four terms of Eq.(2) and  $V^\sigma(t)$  corresponds to all the other terms of the Hamiltonian defined in eq.(5). Then, by substituting eq.(5) in eq.(9), we get,

$$\begin{aligned} \tilde{V}^\sigma(t) &= \tilde{V}_{12}^\sigma(t) C_1^{\sigma\dagger}(t) C_2^\sigma(t) + \tilde{V}_{21}^\sigma(t) C_2^{\sigma\dagger}(t) C_1^\sigma(t) \\ &+ \sum_{K_L} [\tilde{V}_{1K_L}^\sigma(t) C_1^{\sigma\dagger}(t) C_{K_L}^\sigma(t) + \tilde{V}_{K_L 1}^\sigma(t) C_{K_L}^{\sigma\dagger}(t) C_1^\sigma(t)] \\ &+ \sum_{K_R} [\tilde{V}_{1K_R}^\sigma(t) C_1^{\sigma\dagger}(t) C_{K_R}^\sigma(t) + \tilde{V}_{K_R 1}^\sigma(t) C_{K_R}^{\sigma\dagger}(t) C_1^\sigma(t)] \end{aligned} \quad (9)$$

$$\tilde{V}_{ij}^{\sigma'}(t) \text{ are defined by, } \langle i\sigma | \tilde{V}(t) | j\sigma' \rangle = \delta_{\sigma\sigma'} \langle i\sigma | \tilde{V}^\sigma(t) | j\sigma \rangle \quad (10)$$

The electron occupancy of the main quantum dot  $n_1^\sigma(t)$  and the side coupled quantum dot  $n_2^\sigma(t)$  with the spin  $\sigma$ , by using the time evolution operator technique, can be given in terms of the appropriate matrix elements of the evolution operator [29,32,33]:

$$\begin{aligned} n_1^\sigma(t) &= n_1^\sigma(t_0) |U_{1\sigma,1\sigma}(t, t_0)|^2 + n_2^\sigma(t_0) |U_{1\sigma,2\sigma}(t, t_0)|^2 \\ &+ \sum_{K_L} n_{K_L}^\sigma(t_0) |U_{1\sigma,K_L\sigma}(t, t_0)|^2 + \sum_{K_R} n_{K_R}^\sigma(t_0) |U_{1\sigma,K_R\sigma}(t, t_0)|^2 \end{aligned} \quad (11)$$

and ,



$$n_2^\sigma(t) = n_2^\sigma(t_0) |U_{2\sigma,2\sigma}(t, t_0)|^2 + n_1^\sigma(t_0) |U_{2\sigma,1\sigma}(t, t_0)|^2 + \sum_{k_L} n_{k_L}^\sigma(t_0) |U_{2\sigma,k_L\sigma}(t, t_0)|^2 + \sum_{k_R} n_{k_R}^\sigma(t_0) |U_{2\sigma,k_R\sigma}(t, t_0)|^2 \quad (12)$$

With  $n_1^\sigma(t_0)$ ,  $n_2^\sigma(t_0)$ ,  $n_{k_L}^\sigma(t_0)$  and  $n_{k_R}^\sigma(t_0)$  denote the initial occupancy of the main quantum dot, side coupled quantum dot, and left and right leads, respectively.  $U_{i\sigma,j\sigma}(t, t_0) = \langle i\sigma | U(t, t_0) | j\sigma \rangle$  are the appropriate matrix elements of the operator  $U(t, t_0)$ .  $|i\sigma\rangle$  and  $|j\sigma\rangle$  belong to the operator of basis functions  $\{ |1\sigma\rangle, |2\sigma\rangle, |k_L\sigma\rangle \text{ and } |k_R\sigma\rangle \}$ .

It follows from eq.(11) and eq.(12) that in order to calculate the occupation numbers  $n_1^\sigma(t)$  and  $n_2^\sigma(t)$  we have to calculate the matrix elements  $U_{1\sigma,1\sigma}(t, t_0)$ ,  $U_{1\sigma,2\sigma}(t, t_0)$ ,  $U_{2\sigma,2\sigma}(t, t_0)$ ,  $U_{2\sigma,1\sigma}(t, t_0)$ ,  $U_{i\sigma,k_\alpha\sigma}(t, t_0)$  and  $U_{k_\alpha\sigma,i\sigma}(t, t_0)$  with  $i=1,2$  and  $\alpha = L, R$ .

Now, in order to calculate  $U_{1\sigma,1\sigma}(t, t_0)$ , one should construct its equation of motion by writing ,

$$i \frac{\partial}{\partial t} \langle 1\sigma | U(t, t_0) | 1\sigma \rangle = \langle 1\sigma | \tilde{V}^\sigma(t) U(t, t_0) | 1\sigma \rangle \quad (13)$$

Then by using suitable identity operator, after some algebra we get,

$$i \frac{\partial}{\partial t} U_{1\sigma,1\sigma}(t, t_0) = \tilde{V}_{12}^\sigma(t) U_{2\sigma,1\sigma}(t, t_0) + \sum_{k_L} \tilde{V}_{1k_L}^\sigma(t) U_{k_L\sigma,1\sigma}(t, t_0) + \sum_{k_R} \tilde{V}_{1k_R}^\sigma(t) U_{k_R\sigma,1\sigma}(t, t_0) \quad (14)$$

The mathematical steps, that are concerned to the terms in the right side of eq.(14), are introduced in table (1). The symbol ( \_\_\_\_\_ ) means that the process of creation or annihilation is not valid. The algebra that must be performed to derive the equations of motion for these time evolution operators matrix elements are presented in tables (1- 4). Then, by using the same algebra steps we get the other equations of motion for the required time evolution operators.

**Table (1) : The matrix elements  $\langle 1\sigma | \tilde{V}^\sigma(t) | j\sigma \rangle$  where  $j = 1\sigma, 2\sigma, k_L\sigma, k_R\sigma$**

Ket Bra	$ 1\sigma\rangle$	$ 2\sigma\rangle$	$\sum_{k'_L}  k'_L\sigma\rangle$	$\sum_{k'_R}  k'_R\sigma\rangle$
$\langle 1\sigma   \tilde{V}_{12}^\sigma(t) C_{1\sigma}^+(t) C_{2\sigma}(t)$	—	$\tilde{V}_{12}^\sigma(t) \langle 1\sigma   1\sigma \rangle$ $= \tilde{V}_{12}(t)$	—	—
$\langle 1\sigma   \tilde{V}_{21}^\sigma(t) C_{2\sigma}^+(t) C_{1\sigma}(t)$	$\tilde{V}_{21}^\sigma(t) \langle 1\sigma   2\sigma \rangle$ $= 0$	—	—	—
$\langle 1\sigma   \sum_{k_L} \tilde{V}_{1k_L}^\sigma(t) C_{1\sigma}^+(t) C_{k_L\sigma}(t)$	—	—	$\sum_{k_L} \tilde{V}_{1k_L}^\sigma(t) \langle 1\sigma   1\sigma \rangle$ $= \sum_{k_L} \tilde{V}_{1k_L}^\sigma(t)$	—
$\langle 1\sigma   \sum_{k_L} \tilde{V}_{k_L1}^\sigma(t) C_{k_L\sigma}^+(t) C_{1\sigma}(t)$	$\sum_{k_L} \tilde{V}_{k_L1}^\sigma(t) \langle 1\sigma   k_L\sigma \rangle$ $= 0$	—	—	—
$\langle 1\sigma   \sum_{k_R} \tilde{V}_{1k_R}^\sigma(t) C_{1\sigma}^+(t) C_{k_R\sigma}(t)$	—	—	—	$\sum_{k_R} \tilde{V}_{1k_R}^\sigma(t) \langle 1\sigma   1\sigma \rangle$ $= \sum_{k_R} \tilde{V}_{1k_R}^\sigma(t)$
$\langle 1\sigma   \sum_{k_R} \tilde{V}_{k_R1}^\sigma(t) C_{k_R\sigma}^+(t) C_{1\sigma}(t)$	$\sum_{k_R} \tilde{V}_{k_R1}^\sigma(t) \langle 1\sigma   k_R\sigma \rangle$ $= 0$	—	—	—

**Table (2) : The matrix elements  $\langle 2\sigma | \tilde{V}^\sigma(t) | j\sigma \rangle$  where  $j = 1\sigma, 2\sigma, k_L\sigma, k_R\sigma$**

Ket Bra	$ 1\sigma\rangle$	$ 2\sigma\rangle$	$\sum_{k'_L}  k'_L\sigma\rangle$	$\sum_{k'_R}  k'_R\sigma\rangle$
$\langle 2\sigma   \tilde{V}_{12}^\sigma(t) C_{1\sigma}^+(t) C_{2\sigma}(t)$	—	$\tilde{V}_{12}^\sigma(t) \langle 2\sigma   1\sigma \rangle$ $= 0$	—	—
$\langle 2\sigma   \tilde{V}_{21}^\sigma(t) C_{2\sigma}^+(t) C_{1\sigma}(t)$	$\tilde{V}_{21}^\sigma(t) \langle 2\sigma   2\sigma \rangle$ $= \tilde{V}_{21}(t)$	—	—	—
$\langle 2\sigma   \sum_{k_L} \tilde{V}_{1k_L}^\sigma(t) C_{1\sigma}^+(t) C_{k_L\sigma}(t)$	—	—	$\sum_{k_L} \tilde{V}_{1k_L}^\sigma(t) \langle 2\sigma   1\sigma \rangle$ $= 0$	—
$\langle 2\sigma   \sum_{k_L} \tilde{V}_{k_L1}^\sigma(t) C_{k_L\sigma}^+(t) C_{1\sigma}(t)$	$\sum_{k_L} \tilde{V}_{k_L1}^\sigma(t) \langle 2\sigma   k_L\sigma \rangle$ $= 0$	—	—	—
$\langle 2\sigma   \sum_{k_R} \tilde{V}_{1k_R}^\sigma(t) C_{1\sigma}^+(t) C_{k_R\sigma}(t)$	—	—	—	$\sum_{k_R} \tilde{V}_{1k_R}^\sigma(t) \langle 2\sigma   1\sigma \rangle$ $= 0$
$\langle 2\sigma   \sum_{k_R} \tilde{V}_{k_R1}^\sigma(t) C_{k_R\sigma}^+(t) C_{1\sigma}(t)$	$\sum_{k_R} \tilde{V}_{k_R1}^\sigma(t) \langle 2\sigma   k_R\sigma \rangle$ $= 0$	—	—	—

**Table (3): The matrix elements  $\langle k_L''\sigma | \tilde{V}^\sigma(t) | j\sigma \rangle$  where  $j = 1\sigma, 2\sigma, k_L\sigma, k_R\sigma$**

Ket \ Bra	Ket			
	$ 1\sigma\rangle$	$ 2\sigma\rangle$	$\sum_{k_L}  k_L'\sigma\rangle$	$\sum_{k_R}  k_R'\sigma\rangle$
$\langle k_L''\sigma   \tilde{V}_{12}^\sigma(t) C_{1\sigma}^+(t) C_{2\sigma}(t)$	—	$\tilde{V}_{12}^\sigma(t) \langle k_L''\sigma   1\sigma \rangle = 0$	—	—
$\langle k_L''\sigma   \tilde{V}_{21}^\sigma(t) C_{2\sigma}^+(t) C_{1\sigma}(t)$	$\tilde{V}_{21}^\sigma(t) \langle k_L''\sigma   2\sigma \rangle = 0$	—	—	—
$\langle k_L''\sigma   \sum_{k_L} \tilde{V}_{1k_L}^\sigma(t) C_{1\sigma}^+(t) C_{k_L\sigma}(t)$	—	—	$\sum_{k_L} \tilde{V}_{1k_L}^\sigma(t) \langle k_L''\sigma   1\sigma \rangle = 0$	—
$\langle k_L''\sigma   \sum_{k_L} \tilde{V}_{k_L 1}^\sigma(t) C_{k_L\sigma}^+(t) C_{1\sigma}(t)$	$\sum_{k_L} \tilde{V}_{k_L 1}^\sigma(t) \langle k_L''\sigma   k_L\sigma \rangle = \tilde{V}_{k_L' 1}^\sigma(t)$	—	—	—
$\langle k_L''\sigma   \sum_{k_R} \tilde{V}_{1k_R}^\sigma(t) C_{1\sigma}^+(t) C_{k_R\sigma}(t)$	—	—	—	$\sum_{k_R} \tilde{V}_{1k_R}^\sigma(t) \langle k_L''\sigma   1\sigma \rangle = 0$
$\langle k_L''\sigma   \sum_{k_R} \tilde{V}_{k_R 1}^\sigma(t) C_{k_R\sigma}^+(t) C_{1\sigma}(t)$	$\sum_{k_R} \tilde{V}_{k_R 1}^\sigma(t) \langle k_L''\sigma   k_R\sigma \rangle = 0$	—	—	—

**Table (4) : The matrix elements  $\langle k_R''\sigma | \tilde{V}^\sigma(t) | j\sigma \rangle$  where  $j = 1\sigma, 2\sigma, k_L\sigma, k_R\sigma$**

Ket \ Bra	Ket			
	$ 1\sigma\rangle$	$ 2\sigma\rangle$	$\sum_{k_L}  k_L'\sigma\rangle$	$\sum_{k_R}  k_R'\sigma\rangle$
$\langle k_R''\sigma   \tilde{V}_{12}^\sigma(t) C_{1\sigma}^+(t) C_{2\sigma}(t)$	—	$\tilde{V}_{12}^\sigma(t) \langle k_R''\sigma   1\sigma \rangle = 0$	—	—
$\langle k_R''\sigma   \tilde{V}_{21}^\sigma(t) C_{2\sigma}^+(t) C_{1\sigma}(t)$	$\tilde{V}_{21}^\sigma(t) \langle k_R''\sigma   2\sigma \rangle = 0$	—	—	—
$\langle k_R''\sigma   \sum_{k_L} \tilde{V}_{1k_L}^\sigma(t) C_{1\sigma}^+(t) C_{k_L\sigma}(t)$	—	—	$\sum_{k_L} \tilde{V}_{1k_L}^\sigma(t) \langle k_R''\sigma   1\sigma \rangle = 0$	—
$\langle k_R''\sigma   \sum_{k_L} \tilde{V}_{k_L 1}^\sigma(t) C_{k_L\sigma}^+(t) C_{1\sigma}(t)$	$\sum_{k_L} \tilde{V}_{k_L 1}^\sigma(t) \langle k_R''\sigma   k_L\sigma \rangle = 0$	—	—	—
$\langle k_R''\sigma   \sum_{k_R} \tilde{V}_{1k_R}^\sigma(t) C_{1\sigma}^+(t) C_{k_R\sigma}(t)$	—	—	—	$\sum_{k_R} \tilde{V}_{1k_R}^\sigma(t) \langle k_R''\sigma   1\sigma \rangle = 0$
$\langle k_R''\sigma   \sum_{k_R} \tilde{V}_{k_R 1}^\sigma(t) C_{k_R\sigma}^+(t) C_{1\sigma}(t)$	$\sum_{k_R} \tilde{V}_{k_R 1}^\sigma(t) \langle k_R''\sigma   k_R\sigma \rangle = \tilde{V}_{k_R' 1}^\sigma(t)$	—	—	—

Now, in order to incorporate the electronic properties of the leads, we introduce the following definitions, [34],

$$\begin{aligned} \tilde{V}_{ik_\alpha}^\sigma(t) &= v_{k_\alpha}^\sigma V_{i\alpha}^\sigma(t) \\ \tilde{V}_{k_\alpha i}^\sigma(t) &= v_{k_\alpha}^{*\sigma} V_{\alpha i}^\sigma(t) \end{aligned} \quad (15)$$

And we also define the following relations as follows:

$$\begin{aligned} U_{k_\alpha\sigma, i\sigma}(t, t_0) &= v_{k_\alpha}^{*\sigma} U_{\alpha\sigma, i\sigma}(t, t_0) \\ U_{i\sigma, k_\alpha\sigma}(t, t_0) &= v_{k_\alpha}^\sigma U_{i\sigma, \alpha\sigma}(t, t_0) \end{aligned} \quad (16)$$

And,

$$U_{k_L\sigma, k_R\sigma}(t, t_0) = v_{k_L}^{*\sigma} v_{k_R}^\sigma U_{L\sigma, R\sigma}(t, t_0) \quad (17)$$

The general formula of the lead density of states is given by [35],

$$\rho_\alpha^\sigma(E^\sigma) = \sum_{k_\alpha} |v_{k_\alpha}^\sigma|^2 \delta(E - E_{k_\alpha}^\sigma) \quad \alpha = L, R \quad (18)$$

with [36],

$$\int_{-\infty}^{+\infty} \delta(E - E_{k_\alpha}^\sigma) dE = 1 \quad (19)$$

By substituting the above mentioned relations eqs.(15-17) in the equations of motion and by getting use of eq. (18) and eq.(19), we get,

$$\begin{aligned} i \frac{\partial}{\partial t} U_{1\sigma, 1\sigma}(t, t_0) &= V_{12}^\sigma(t) U_{2\sigma, 1\sigma}(t, t_0) \\ &+ \int_{-\infty}^{+\infty} \rho_L^\sigma(E_L^\sigma) V_{1L}^\sigma(t) U_{L\sigma, 1\sigma}(t, t_0) dE_L^\sigma \\ &+ \int_{-\infty}^{+\infty} \rho_R^\sigma(E_R^\sigma) V_{1R}^\sigma(t) U_{R\sigma, 1\sigma}(t, t_0) dE_R^\sigma \end{aligned} \quad (20)$$

$$\begin{aligned} i \frac{\partial}{\partial t} U_{1\sigma, 2\sigma}(t, t_0) &= V_{12}^\sigma(t) U_{2\sigma, 2\sigma}(t, t_0) \\ &+ \int_{-\infty}^{+\infty} \rho_L^\sigma(E_L^\sigma) V_{1L}^\sigma(t) U_{L\sigma, 2\sigma}(t, t_0) dE_L^\sigma \\ &+ \int_{-\infty}^{+\infty} \rho_R^\sigma(E_R^\sigma) V_{1R}^\sigma(t) U_{R\sigma, 2\sigma}(t, t_0) dE_R^\sigma \end{aligned} \quad (21)$$

$$\begin{aligned} i \frac{\partial}{\partial t} U_{1\sigma, L'\sigma}(t, t_0) &= V_{12}^\sigma(t) U_{2\sigma, L'\sigma}(t, t_0) \\ &+ \int_{-\infty}^{+\infty} \rho_L^\sigma(E_L^\sigma) V_{1L}^\sigma(t) U_{L\sigma, L'\sigma}(t, t_0) dE_L^\sigma \\ &+ \int_{-\infty}^{+\infty} \rho_R^\sigma(E_R^\sigma) V_{1R}^\sigma(t) U_{R\sigma, L'\sigma}(t, t_0) dE_R^\sigma \end{aligned} \quad (22)$$



$$\begin{aligned}
 i \frac{\partial}{\partial t} U_{1\sigma, R'\sigma}(t, t_0) &= V_{12}^\sigma(t) U_{2\sigma, R'\sigma}(t, t_0) \\
 &+ \int_{-\infty}^{+\infty} \rho_L^\sigma(E_L^\sigma) V_{1L}^\sigma(t) U_{L\sigma, R'\sigma}(t, t_0) dE_L^\sigma \\
 &+ \int_{-\infty}^{+\infty} \rho_R^\sigma(E_R^\sigma) V_{1R}^\sigma(t) U_{R\sigma, R'\sigma}(t, t_0) dE_R^\sigma \quad (23)
 \end{aligned}$$

$$i \frac{\partial}{\partial t} U_{2\sigma, 2\sigma}(t, t_0) = V_{21}^\sigma(t) U_{1\sigma, 2\sigma}(t, t_0) \quad (24)$$

$$i \frac{\partial}{\partial t} U_{2\sigma, 1\sigma}(t, t_0) = V_{21}^\sigma(t) U_{1\sigma, 1\sigma}(t, t_0) \quad (25)$$

$$i \frac{\partial}{\partial t} U_{L\sigma, 1\sigma}(t, t_0) = V_{L1}^\sigma(t) U_{1\sigma, 1\sigma}(t, t_0) \quad (26)$$

$$i \frac{\partial}{\partial t} U_{R\sigma, 1\sigma}(t, t_0) = V_{R1}^\sigma(t) U_{1\sigma, 1\sigma}(t, t_0) \quad (27)$$

$$i \frac{\partial}{\partial t} U_{L\sigma, 2\sigma}(t, t_0) = V_{L1}^\sigma(t) U_{1\sigma, 2\sigma}(t, t_0) \quad (30)$$

$$i \frac{\partial}{\partial t} U_{R\sigma, 2\sigma}(t, t_0) = V_{R1}^\sigma(t) U_{1\sigma, 2\sigma}(t, t_0) \quad (31)$$

$$i \frac{\partial}{\partial t} U_{2\sigma, L\sigma}(t, t_0) = V_{21}(t) U_{1\sigma, L\sigma}(t, t_0) \quad (30)$$

$$i \frac{\partial}{\partial t} U_{2\sigma, R\sigma}(t, t_0) = V_{21}(t) U_{1\sigma, R\sigma}(t, t_0) \quad (31)$$

$$i \frac{\partial}{\partial t} U_{L'\sigma, L\sigma}(t, t_0) = V_{L'1}^\sigma(t) U_{1\sigma, L\sigma}(t, t_0) \quad (32)$$

$$i \frac{\partial}{\partial t} U_{R'\sigma, R\sigma}(t, t_0) = V_{R'1}^\sigma(t) U_{1\sigma, R\sigma}(t, t_0) \quad (33)$$

$$i \frac{\partial}{\partial t} U_{R\sigma, L\sigma}(t, t_0) = V_{R1}^\sigma(t) U_{1\sigma, L\sigma}(t, t_0) \quad (34)$$

$$i \frac{\partial}{\partial t} U_{L\sigma, R\sigma}(t, t_0) = V_{L1}^\sigma(t) U_{1\sigma, R\sigma}(t, t_0) \quad (35)$$

The knowledge of the matrix elements  $U_{i\sigma, j\sigma}(t, t_0)$  is sufficient to calculate both the charge localized on each quantum dot and the current flowing through the system under consideration. In order to simplify the calculations [37] of the occupation number, we introduce the following definition:

$$C_{k_\alpha}^\sigma(t_0) \approx \sqrt{f_\alpha^\sigma(E_{k_\alpha}^\sigma, T_\alpha)} \quad (36)$$

Where  $f_\alpha^\sigma(E_{k_\alpha}^\sigma, T)$  is the spin dependent Fermi distribution function in the lead  $\alpha$ ,  $T$  is the temperature of the leads.

Accordingly, eq.(11) and eq.(12) are rewritten as:



$$\begin{aligned}
 n_1^\sigma(t) &= n_1^\sigma(t_0) |U_{1\sigma,1\sigma}(t, t_0)|^2 + n_2^\sigma(t_0) |U_{1\sigma,2\sigma}(t, t_0)|^2 \\
 &+ \int dE_L^\sigma \rho_L^\sigma(E_L^\sigma) f_L^\sigma(E_L^\sigma, T) |U_{1\sigma,L\sigma}(t, t_0)|^2 \\
 &+ \int dE_R^\sigma \rho_R^\sigma(E_R^\sigma) f_R^\sigma(E_R^\sigma, T) |U_{1\sigma,R\sigma}(t, t_0)|^2
 \end{aligned} \tag{37}$$

and,

$$\begin{aligned}
 n_2^\sigma(t) &= n_2^\sigma(t_0) |U_{2\sigma,2\sigma}(t, t_0)|^2 + n_1^\sigma(t_0) |U_{2\sigma,1\sigma}(t, t_0)|^2 \\
 &+ \int dE_L^\sigma \rho_L^\sigma(E_L^\sigma) f_L^\sigma(E_L^\sigma, T) |U_{2\sigma,L\sigma}(t, t_0)|^2 \\
 &+ \int dE_R^\sigma \rho_R^\sigma(E_R^\sigma) f_R^\sigma(E_R^\sigma, T) |U_{2\sigma,R\sigma}(t, t_0)|^2
 \end{aligned} \tag{38}$$

The tunneling current flowing from the left lead  $I_L^\sigma(t)$  can be obtained by using the time derivative of the total number of electrons in the left lead  $n_L^\sigma$  [38, 39],

$$I_L^\sigma = -e \frac{dn_L^\sigma}{dt} \tag{39}$$

And by using the same procedure, we get,

$$\begin{aligned}
 n_L^\sigma(t) &= \iint dE_L^\sigma dE_{L'}^\sigma f^\sigma(E_{L'}^\sigma, T) \rho_L^\sigma(E_L^\sigma) \rho_{L'}^\sigma(E_{L'}^\sigma) |U_{L\sigma,L'\sigma}(t, t_0)|^2 \\
 &+ \iint dE_L^\sigma dE_R^\sigma f^\sigma(E_R^\sigma, T) \rho_L^\sigma(E_L^\sigma) \rho_R^\sigma(E_R^\sigma) |U_{L\sigma,R\sigma}(t, t_0)|^2 \\
 &+ \int dE_L^\sigma n_1^\sigma(t_0) \rho_L^\sigma(E_L^\sigma) |U_{L\sigma,1\sigma}(t, t_0)|^2 \\
 &+ \int dE_L^\sigma n_2^\sigma(t_0) \rho_L^\sigma(E_L^\sigma) |U_{L\sigma,2\sigma}(t, t_0)|^2
 \end{aligned} \tag{40}$$

In our treatment, the system is driven out of equilibrium by applying external time dependent field. It is assumed that the system considered in our treatment is described (within adiabatic approximation) by:

$$E_{k\alpha}^\sigma(t) = E_{k\alpha}^\sigma + \Delta_\alpha \cos \omega t \quad (\alpha = L, R) \tag{41}$$

$$E_{di}^\sigma(t) = E_{di}^\sigma + \Delta_i \cos \omega t \quad (i=1,2) \tag{42}$$

Which means that the spin dependent levels of the leads and the quantum dots are driven by the external time dependent field with the frequency  $\omega$  and the amplitudes  $\Delta_\alpha$  and  $\Delta_i$ , respectively [25].

Therefore, our treatment is concerned with the elastic current in which electrons emit or absorb photons as a virtual process [40]. So, accordingly the spin dependent coupling interactions between the subsystem due to external time dependent field is given by [41].

$$\tilde{V}_{mn}^\sigma(\mathbf{t}) = V_{nm}^\sigma \exp(i(\mathbf{E}_m^\sigma - \mathbf{E}_n^\sigma)(\mathbf{t} - \mathbf{t}_0)) \exp\left(i \frac{\Delta_m - \Delta_n}{\omega} (\sin(\omega \mathbf{t}) - \sin(\omega \mathbf{t}_0))\right)$$

$$\text{With } m, n = 1, 2, k_L, k_R \tag{43}$$

Finally, as the leads considered in our treatment are ferromagnetic, extended theoretical treatment will be presented in the following section to introduce the method used to calculate the density of states of the leads.

### 3 - First-principles Study on the Half-metallic Ferromagnetism of Zinc-blende Structural ScSn

The first-principles calculations based on the density functional theory accomplished in the Wien 2K code are exploited to examine the magnetic and electronic characteristic of the bulk ScSn. The equilibrium lattice constant of bulk ScSn is equal 0.6697 nm. The mesh which has used for the bulk is  $14 \times 14 \times 14$  k meshes. Furthermore, the expansion was set up to be  $I=10$  and  $R_{mt} \times K_{max}$  was equal to 8.0 in the muffin tins. In this study, the spin-orbital coupling was neglected since it has a trivial effect on the main findings. The radii  $R_{mt}$  of the muffin-tin spheres in respective has set to the radii  $R_{mt}$  of the muffin-tin spheres in respective have set to be 2.21 a.u. 1.96 a.u. of Sc and Sn atoms for the bulk. The self-correspondence of the overall energy variation between succeeding repetitions has been accomplished with a precision less than  $10^{-5}$  Ry per formula unit.

This work has focused on the geometry developments of the lattice constants of bulk ScSn, by applying the ferromagnetic measurements of respective total energy vs lattice constants curves, as shown in fig.(2). Therefore, the equilibrium lattice constant has been acquired from the smallest energy. Results was showed that the measured equilibrium lattice constant of ScSn is 0.6697 nm. Although there are no available experimental data to compare our findings with studies on FM HM of ZB TM pnictides, and chalcogenides. Results have revealed that the ZB structure have no lowest total energy when compared with other crystal lattices. Nevertheless, the ZB films of CrAs and CrSb were manufactured from suitable ZB semiconducting materials [42-45]. The calculated total magnetic moment, the magnetic moments of the Sc, Sn and total have been given as a function of the lattice constant as showed in Fig.(3). It is clear that the bulk has ScSn total magnetic moment amounting to  $1 \mu_B$  per formula unit; this value agrees with results of Reference [46].

The calculated total magnetic moment has followed the Slater-Paulig rule of the binary materials: [47]

$$M_{tot} = (Z_{tot} - 8) \mu_B \quad (44)$$

$M_{tot}$  represents the total magnetic moment per formula unit and the  $Z_{tot}$  denotes the total number of valence electrons. In ZB ScSn, the valence band contains seven electrons (Sc:  $4s^2, 3d^1$ ) and (Sn:  $5s^2, 5p^2$ ). Thus, the number of electrons in each shell is equal to 7 and this implies that the total magnetic moments are equal to  $1 \mu_B$  per formula unit which is the integer value. The integer value is considered one of the most important conditions and requirements of substances to be HM ferromagnetic. The total magnetic moment of ScSn contains two portions: the total magnetic moment of the Sc atom ( $0.28990 \mu_B$ ) and the Sn atom ( $0.24691 \mu_B$ ), the main contribution to the total spin magnetic moments of ZB ScSn is attributed to the spin polarization of Sc cases.

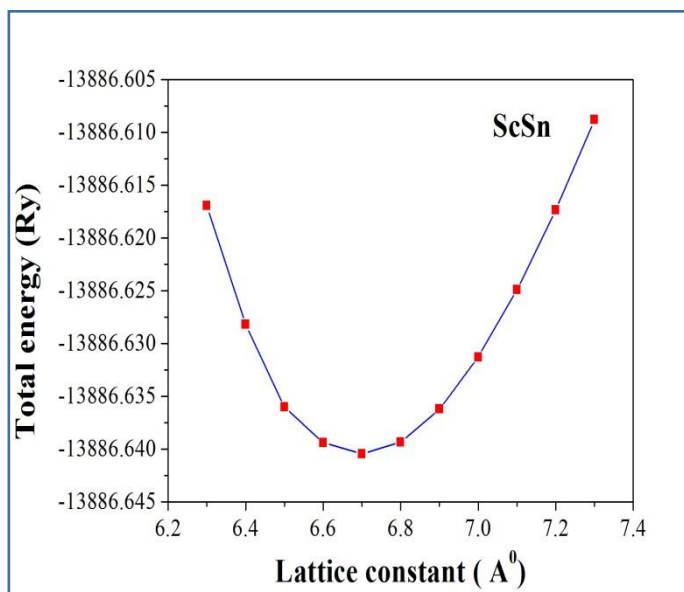


**Fig. (2) Calculated total energy of the ScSn as a function of lattice constant**

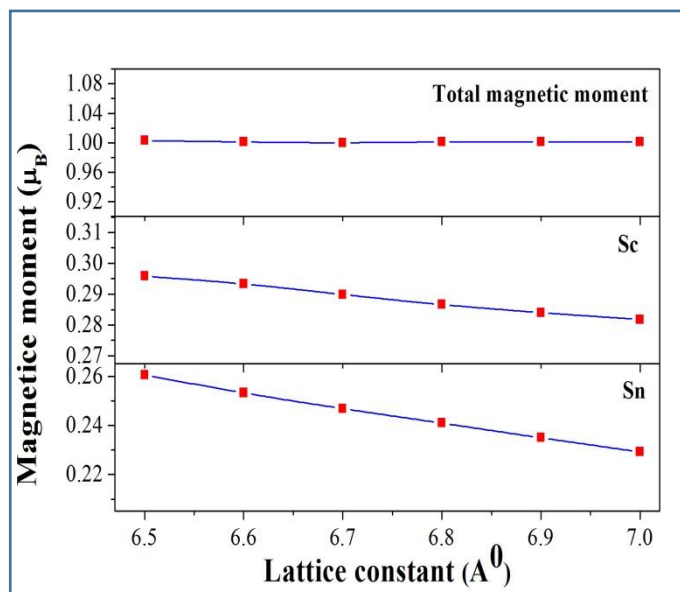


**Fig. (3) The calculated total and partial magnetic moments( $\mu_B$ ) for ScSn**

Fig. (4) shows the spin-polarized total density of states of FM ScSn during this equilibrium lattice constant. The P-state Sn has occupied the area under Fermi level, while the s-state Sn is located about -6 eV below Fermi level and do not appear in the above mentioned figure. The Fermi level has been set to zero and the spin located down was factored by -1. Moreover, it can be seen clearly from Fig.(4) that there are energy gap for the majority spin bands at the Fermi level. The minority spin channel has exhibited metal properties, analogous to the HM of compounds like ZB MnC, MC (M=Ca,Sr, and Ba), CaSi, and CaGe [48]. Thus, ScX materials are considered HM ferromagnets. In addition, one can see that presence of the HM gap [49-53] which can be known as the smallest value between the lowest energy of majority-spin and minority-spin conduction bands relating to Fermi level. For the ScSn compound the HM gap is 0.09 eV and the energy gap is 0.707 eV. These gaps are considered comparatively small when compared with those of other ZB HM compounds. However, it can lead to an increase in Curie temperatures, as it happened with other ZB HM compounds [48].

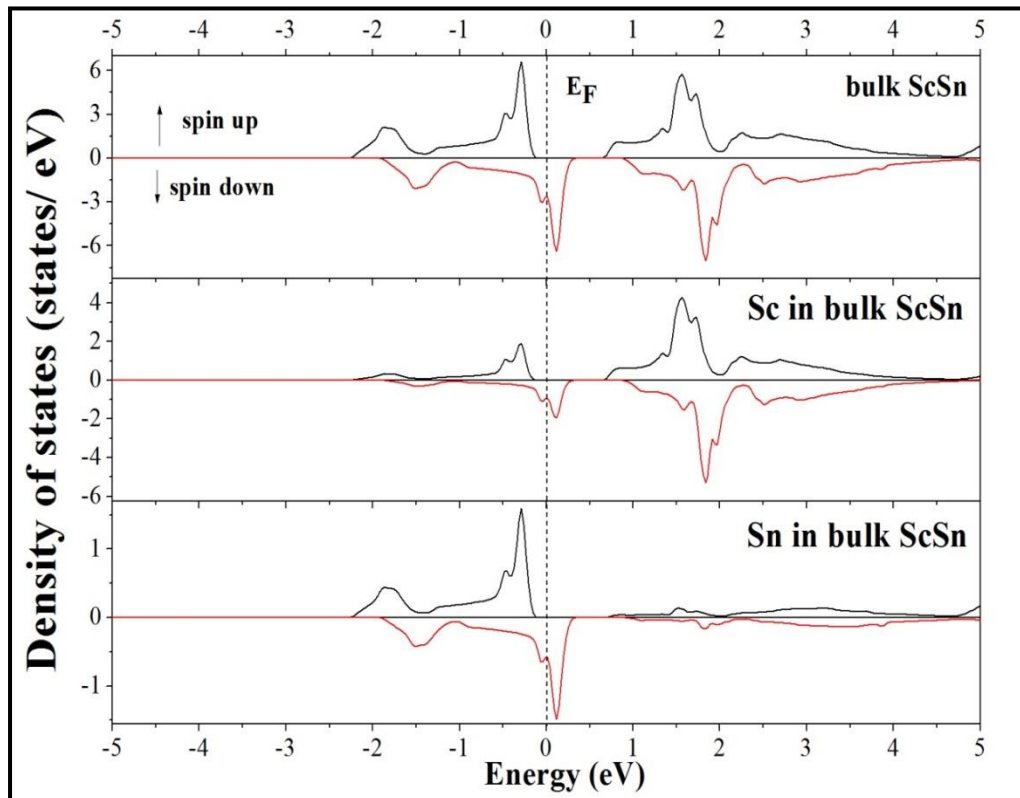


Fig. (4): (a) The total density of states for ScSn, (b and c) the partial density of states for ScSn. Vertical dashed lines points out Fermi level at 0 eV.

#### 4 - Results and Discussion

The related set of integro-differential equations of motion are solved numerically by using six order Runge – Kutta method where the error is checked at each time step with  $\Delta t = 0.1 a.u.$ . The program language used is Fortran 90. The integration over energy is achieved by using Simpson method with  $\Delta E$  is determined according to the leads density of states calculations that presented in section 3. For the case of biased leads, it is assumed that  $\mu_L = -\mu_R$ , where  $\mu_L(\mu_R)$  is the chemical potential of the left (right) lead. The spin dependent quantum dots energy levels are determined by the following:  $E_1^\sigma = E_2^\sigma = -0.5$  eV and  $E_1^{-\sigma} = E_2^{-\sigma} = 0.5$  eV. This may be controlled by the effect of magnetic field (i.e Zeeman splitting). The dots used in our treatment is symmetric. The external time dependent field parameters are as follows:  $\hbar\omega = 0.1$  eV,  $\Delta_1 = 4$  eV,  $\Delta_2 = 1$  eV,  $\Delta_L = 3$  eV,  $\Delta_R = 0$ . At the initial time  $t=t_0 = 0.0$ , the occupation numbers of the quantum dots  $n_i^\sigma$  ( $i = 1,2$ ) are fixed at 0.5. We also assume that the coupling interactions between the subsystems are spin dependent with  $V_{1\alpha}^\sigma = 0.15$  eV,  $V_{1\alpha}^{-\sigma} = 0.05$  eV,  $V_{12}^\sigma = 0.2$  eV,  $V_{12}^{-\sigma} = 0.1$  eV.

Accordingly, it is easy to compute the occupation numbers of both quantum dots, the occupation number on the left lead and the current flowing through the device (calculated in atomic unit). The case of  $V_{1\alpha}^{+\sigma} > V_{1\alpha}^{-\sigma}$  and  $V_{12}^{+\sigma} > V_{12}^{-\sigma}$  is studied and investigated (see fig. (5)). The case of  $V_{1\alpha}^{-\sigma} > V_{1\alpha}^{+\sigma}$  and  $V_{12}^{-\sigma} > V_{12}^{+\sigma}$  is also studied and investigated (see fig. (6)). It can be seen that



$n_L^{+\sigma} > n_L^{-\sigma}$  which means that the time evolution of states on QD1 and QD2 is not related with the time evolution of states in the left lead. In fig.(7) and fig.(8), the frequency of the external time dependent field is increased,  $\hbar\omega = 1.5$  eV, this increasing makes the occupation numbers oscillate for more time. In all these figs., it is obvious that at each time when  $n_1^{\pm\sigma}$  is maximum,  $n_2^{\pm\sigma}$  is minimum and vice versa.

The model parametrization is achieved for the case of bulk ScSn leads by using the above parameters (see figs. (6 to 8)). The values of the occupation numbers and spin accumulation on the quantum dots are listed in tables ((5-8)) at different time. According to these figs. and tables, one can conclude the most important features which are summarized by the following:-

**First :** Figs.(5 to 8) confirm that the spin accumulation is changed with time when  $\mu_L = -\mu_R = 2$  eV. Keeping in mind that the spin currents are determined by the spin accumulation on the left lead.

**Second :** The spin accumulation becomes higher on both quantum dots by using the ScSn bulk leads for all time. While the type of the accumulated spin is not changed with the density of states of the leads variation because both leads are bulk type see Ref. [54]).

**Third :** for the regime  $V_{1\alpha}^{\sigma} > V_{1\alpha}^{-\sigma}$ ,  $V_{12}^{\sigma} > V_{12}^{-\sigma}$  and  $\hbar\omega = 0.1$  eV (or at  $\hbar\omega = 1.5$  eV), the spin accumulation on the quantum dots take it maximum value at the same time (400 a.u.). while for the second regime  $V_{1\alpha}^{\sigma} < V_{1\alpha}^{-\sigma}$ ,  $V_{12}^{\sigma} < V_{12}^{-\sigma}$  and  $\hbar\omega = 0.1$  eV (or at  $\hbar\omega = 1.5$  eV), the maximum value of spin accumulation on the quantum dots are lying at different times. Notably, as the field frequency increases, the over mentioned different times are more shifted.

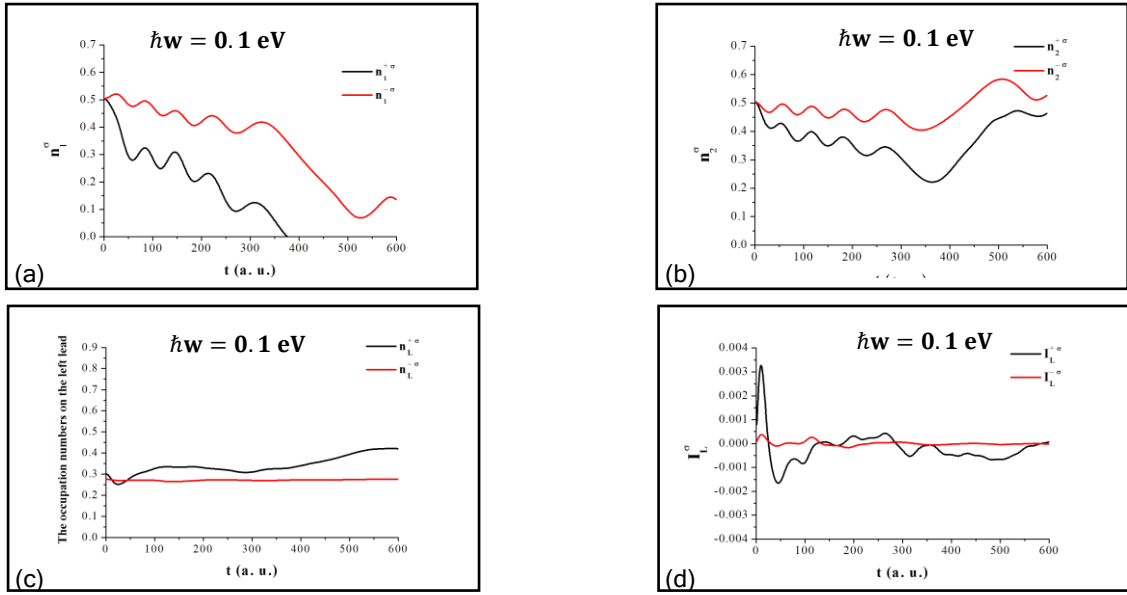


**Fig. (5):** The occupation numbers of (a) main quantum dot (QD1), (b) side quantum dot (QD2), (c) the left lead and (d) the current flowed from the left lead as a function of time , when

$$\begin{aligned}
 &V_{1L}^{\sigma} = V_{1R}^{\sigma} = 0.15 \text{ eV}, V_{1L}^{-\sigma} = V_{1R}^{-\sigma} = 0.05 \text{ eV} \\
 &\Delta_1 = 4 \text{ eV}, \Delta_2 = 1 \text{ eV}, \Delta_L = 3 \text{ eV}, \Delta_R = 0 \text{ eV} \\
 &V_{12}^{+\sigma} = V_{21}^{+\sigma} = 0.2 \text{ eV}, V_{12}^{-\sigma} = V_{21}^{-\sigma} = 0.1 \text{ eV} \\
 &E_1^{+\sigma} = E_2^{+\sigma} = -0.5 \text{ eV}, E_1^{-\sigma} = E_2^{-\sigma} = 0.5 \text{ eV} \\
 &\mu_L = 2 \text{ eV}, \mu_R = -2 \text{ eV}
 \end{aligned}$$

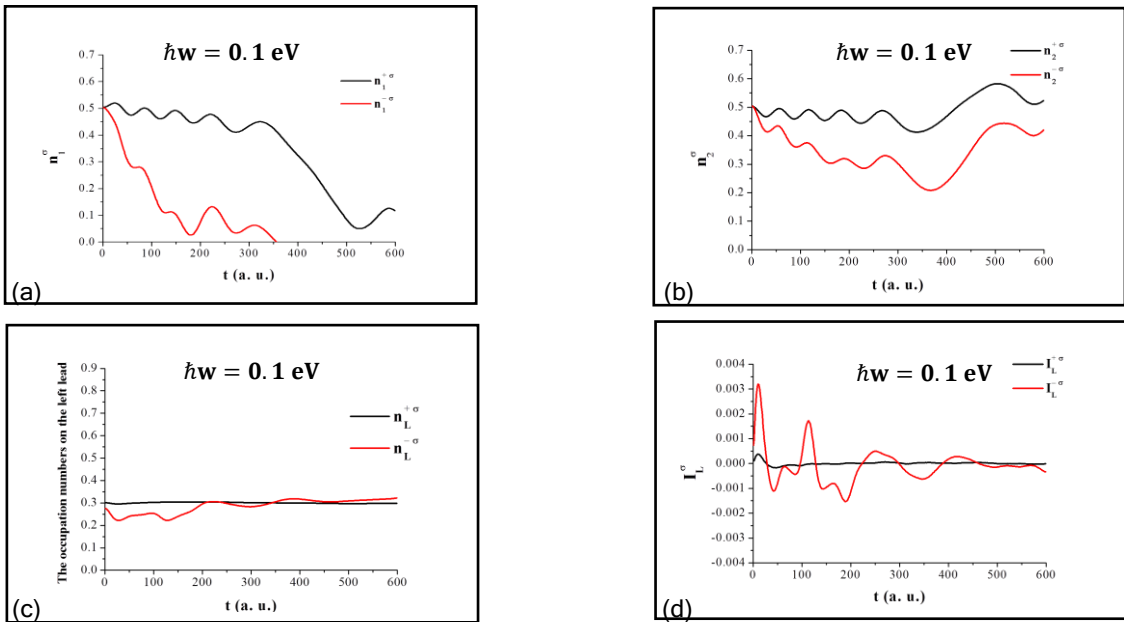


**Fig. (6):** The occupation numbers of (a) main quantum dot (QD1), (b) side quantum dot (QD2), (c) the left lead and (d) the current flowed from the left lead as a function of time , when

$$\begin{aligned}
 &V_{1L}^{\sigma} = V_{1R}^{\sigma} = 0.05 \text{ eV}, V_{1L}^{-\sigma} = V_{1R}^{-\sigma} = 0.15 \text{ eV} \\
 &\Delta_1 = 4 \text{ eV}, \Delta_2 = 1 \text{ eV}, \Delta_L = 3 \text{ eV}, \Delta_R = 0 \text{ eV} \\
 &V_{12}^{+\sigma} = V_{21}^{+\sigma} = 0.1 \text{ eV}, V_{12}^{-\sigma} = V_{21}^{-\sigma} = 0.2 \text{ eV} \\
 &E_1^{+\sigma} = E_2^{+\sigma} = -0.5 \text{ eV}, E_1^{-\sigma} = E_2^{-\sigma} = 0.5 \text{ eV} \\
 &\mu_L = 2 \text{ eV}, \mu_R = -2 \text{ eV}
 \end{aligned}$$

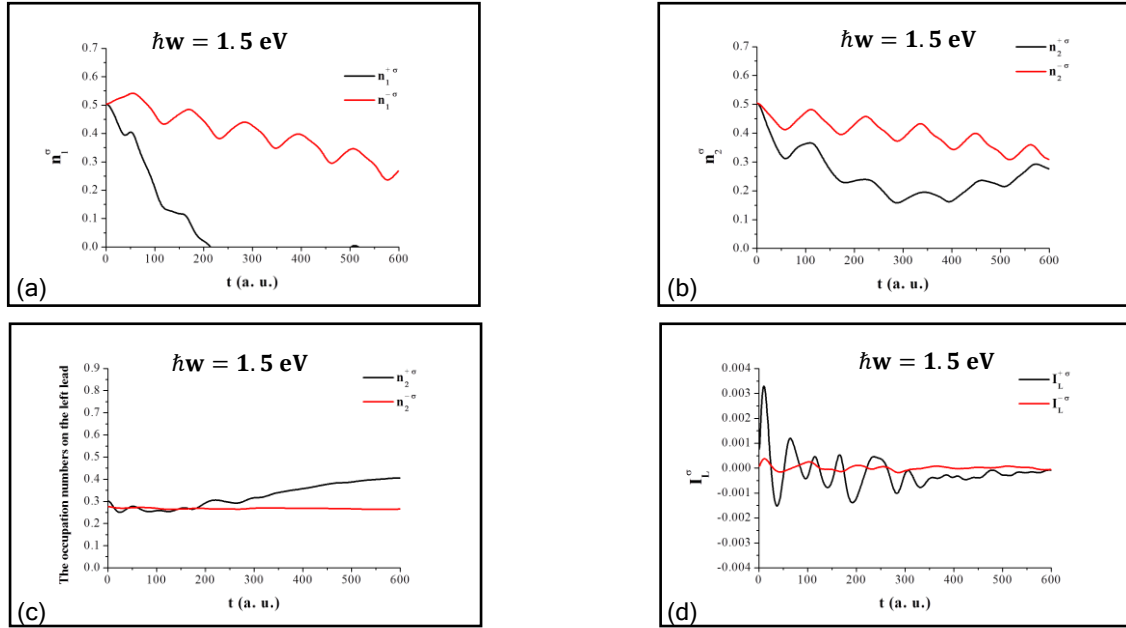


**Fig. (7):** The occupation numbers of (a) main quantum dot (QD1), (b) side quantum dot (QD2), (c) the left lead and (d) the current flowed from the left lead as a function of time , when

$$\begin{aligned}
 V_{1L}^{\sigma} &= V_{1R}^{\sigma} = 0.15 \text{ eV}, & V_{1L}^{-\sigma} &= V_{1R}^{-\sigma} = 0.05 \text{ eV} \\
 \Delta_1 &= 4 \text{ eV}, \Delta_2 = 1 \text{ eV}, & \Delta_L &= 3 \text{ eV}, \Delta_R = 0 \text{ eV} \\
 V_{12}^{+\sigma} &= V_{21}^{+\sigma} = 0.2 \text{ eV}, & V_{12}^{-\sigma} &= V_{21}^{-\sigma} = 0.1 \text{ eV} \\
 E_1^{+\sigma} &= E_2^{+\sigma} = -0.5 \text{ eV}, & E_1^{-\sigma} &= E_2^{-\sigma} = 0.5 \text{ eV} \\
 \mu_L &= 2 \text{ eV}, \mu_R &= -2 \text{ eV}
 \end{aligned}$$

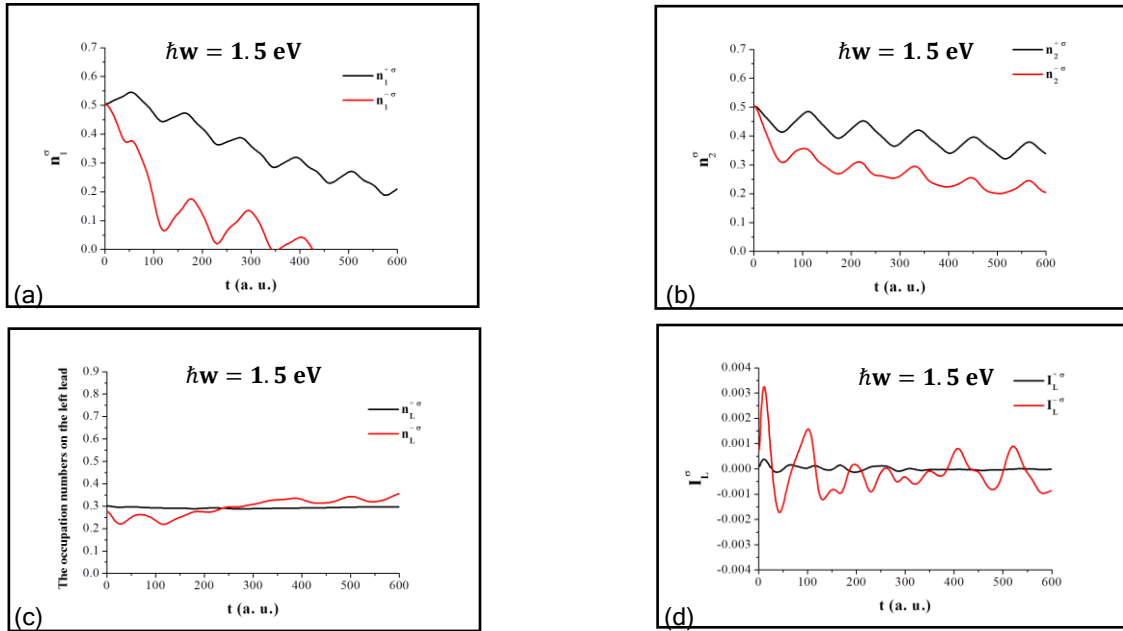


**Fig. (8):** The occupation numbers of (a) main quantum dot (QD1), (b) side quantum dot (QD2), (c) the left lead and (d) the current flowed from the left lead as a function of time , when

$$\begin{aligned}
 V_{1L}^{\sigma} &= V_{1R}^{\sigma} = 0.05 \text{ eV}, & V_{1L}^{-\sigma} &= V_{1R}^{-\sigma} = 0.15 \text{ eV} \\
 \Delta_1 &= 4 \text{ eV}, \Delta_2 = 1 \text{ eV}, & \Delta_L &= 3 \text{ eV}, \Delta_R = 0 \text{ eV} \\
 V_{12}^{+\sigma} &= V_{21}^{+\sigma} = 0.1 \text{ eV}, & V_{12}^{-\sigma} &= V_{21}^{-\sigma} = 0.2 \text{ eV} \\
 E_1^{+\sigma} &= E_2^{+\sigma} = -0.5 \text{ eV}, & E_1^{-\sigma} &= E_2^{-\sigma} = 0.5 \text{ eV} \\
 \mu_L &= 2 \text{ eV}, \mu_R &= -2 \text{ eV}
 \end{aligned}$$



**Table (5):** The occupation numbers and spin accumulation on the quantum dots at different times for bulk ScSn leads with  $\hbar\omega = 0.1$  eV,  $V_{1L}^{+\sigma} = V_{1R}^{+\sigma} = 0.15$  eV,  $V_{1L}^{-\sigma} = V_{1R}^{-\sigma} = 0.05$  eV,  $V_{12}^{+\sigma} = V_{21}^{+\sigma} = 0.2$  eV,  $V_{12}^{-\sigma} = V_{21}^{-\sigma} = 0.1$  eV,  $E_1^{+\sigma} = E_2^{+\sigma} = -0.5$  eV,  $E_1^{-\sigma} = E_2^{-\sigma} = 0.5$  eV,  $\mu_L = 2$  eV,  $\mu_R = -2$  eV,  $\Delta_1 = 4$  eV,  $\Delta_2 = 1$  eV,  $\Delta_L = 3$  eV and  $\Delta_R = 0$  eV

t (a.u.)	$n_1^{+\sigma}$	$n_1^{-\sigma}$	As1	$n_2^{+\sigma}$	$n_2^{-\sigma}$	As2
100	0.28667	0.47507	-0.18840	0.37751	0.47009	-0.09258
200	0.21691	0.41941	-0.2025	0.35333	0.46186	-0.10854
300	0.12071	0.40229	-0.28159	0.30563	0.44106	-0.13543
400	0	0.29446	-0.29446	0.26011	0.45165	-0.19154
500	0	0.09666	-0.09666	0.44585	0.58271	-0.13686
600	0	0.13590	-0.13590	0.46334	0.52728	-0.06394

**Table (6):** The occupation numbers and spin accumulation on the quantum dots at different times for bulk ScSn leads with  $\hbar\omega = 1.5$  eV,  $V_{1L}^{+\sigma} = V_{1R}^{+\sigma} = 0.15$  eV,  $V_{1L}^{-\sigma} = V_{1R}^{-\sigma} = 0.05$  eV,  $V_{12}^{+\sigma} = V_{21}^{+\sigma} = 0.2$  eV,  $V_{12}^{-\sigma} = V_{21}^{-\sigma} = 0.1$  eV,  $E_1^{+\sigma} = E_2^{+\sigma} = -0.5$  eV,  $E_1^{-\sigma} = E_2^{-\sigma} = 0.5$  eV,  $\mu_L = 2$  eV,  $\mu_R = -2$  eV,  $\Delta_1 = 4$  eV,  $\Delta_2 = 1$  eV,  $\Delta_L = 3$  eV and  $\Delta_R = 0$  eV.

t (a.u.)	$n_1^{+\sigma}$	$n_1^{-\sigma}$	As1	$n_2^{+\sigma}$	$n_2^{-\sigma}$	As2
100	0.20852	0.46732	-0.25879	0.36291	0.47211	-0.10920
200	0.02092	0.44459	-0.42368	0.23416	0.42989	-0.19573
300	0	0.42779	-0.42779	0.16516	0.38279	-0.21763
400	0	0.39625	-0.39625	0.16417	0.34448	-0.18032
500	0	0.34373	-0.34373	0.2176	0.33093	-0.11333
600	0	0.26771	-0.26771	0.27618	0.30876	-0.03257

**Table (7):** The occupation numbers and spin accumulation on the quantum dots at different times for bulk ScSn leads with  $\hbar\omega = 0.1$  eV,  $V_{1L}^{+\sigma} = V_{1R}^{+\sigma} = 0.05$  eV,  $V_{1L}^{-\sigma} = V_{1R}^{-\sigma} = 0.15$  eV,  $V_{12}^{+\sigma} = V_{21}^{+\sigma} = 0.1$  eV,  $V_{12}^{-\sigma} = V_{21}^{-\sigma} = 0.2$  eV,  $E_1^{+\sigma} = E_2^{+\sigma} = -0.5$  eV,  $E_1^{-\sigma} = E_2^{-\sigma} = 0.5$  eV,  $\mu_L = 2$  eV,  $\mu_R = -2$  eV,  $\Delta_1 = 4$  eV,  $\Delta_2 = 1$  eV,  $\Delta_L = 3$  eV and  $\Delta_R = 0$  eV

t (a.u.)	$n_1^{+\sigma}$	$n_1^{-\sigma}$	As1	$n_2^{+\sigma}$	$n_2^{-\sigma}$	As2
100	0.48505	0.20633	0.27872	0.47121	0.36510	0.10611
200	0.45709	0.07431	0.38277	0.47194	0.31423	0.15771
300	0.43437	0.05769	0.37668	0.44818	0.30237	0.14581
400	0.32473	0	0.32473	0.46830	0.23747	0.23083
500	0.08464	0	0.08464	0.58220	0.43881	0.14339
600	0.11786	0	0.11786	0.52327	0.42022	0.10305

**Table (8): The occupation numbers and spin accumulation on the quantum dots at different times for bulk ScSn leads with  $\hbar\omega = 1.5$  eV,  $V_{1L}^{+\sigma} = V_{1R}^{+\sigma} = 0.05$  eV,  $V_{1L}^{-\sigma} = V_{1R}^{-\sigma} = 0.15$  eV,  $V_{12}^{+\sigma} = V_{21}^{+\sigma} = 0.1$  eV,  $V_{12}^{-\sigma} = V_{21}^{-\sigma} = 0.2$  eV,  $E_1^{+\sigma} = E_2^{+\sigma} = -0.5$  eV,  $E_1^{-\sigma} = E_2^{-\sigma} = 0.5$  eV,  $\mu_L = 2$  eV,  $\mu_R = -2$  eV,  $\Delta_1 = 4$  eV,  $\Delta_2 = 1$  eV,  $\Delta_L = 3$  eV and  $\Delta_R = 0$  eV.**

t (a.u.)	$n_1^{+\sigma}$	$n_1^{-\sigma}$	As1	$n_2^{+\sigma}$	$n_2^{-\sigma}$	As2
100	0.47256	0.17538	0.29718	0.47376	0.35579	0.11797
200	0.42026	0.12315	0.29711	0.42398	0.29660	0.12738
300	0.35876	0.13128	0.22748	0.37374	0.26104	0.11270
400	0.31455	0.04168	0.27286	0.34075	0.22384	0.11691
500	0.26807	0	0.26807	0.33754	0.20102	0.13652
600	0.20943	0	0.20943	0.33923	0.20423	0.13501

## 5 - Conclusions

According to our extended calculations we report the following conclusions. Increasing the frequency of the fields makes the occupation numbers oscillate for more time. Furthermore, the spin accumulation calculations give physical notes about the tunneling process of the electrons with spin up and spin down. At each time, the tunneling process occurs for spin up electron and spin down electron because both spin channels are available. As the frequency of the external time dependent fields increases, the spin accumulation on both quantum dots is assisted. While the type of accumulated spin is determined by the spin dependent interdot coupling interaction. Moreover, the quantum beats can be controlled by increasing the interdot coupling between the quantum dots. In addition, in spite of the chemical potential  $\mu_L$  is higher than  $\mu_R$  all the time, it is interesting to notice that the time – dependent spin currents become negative for a certain period of time. This behavior does not occur for a classical system and it is an essential feature of the mesoscopic system which is due to the phase coherence. Finally, we anticipate that these findings are helpful in exploiting the spin dependent interdot coupling interaction in spintronics, such as exploiting the quantum computing devices.

## 6 - References

- [1] J. Y. Bai, Z. L. He, S. B. Yang, Acta Phys. Sin. 63, 017303 (2014).
- [2] Z. L. He, T. Q. Lü, Phys. Lett. A 376, 2501 (2012).
- [3] Y. T. Zhang, F. Zhai, Z. H. Qiao, Q. F. Sun, Phys. Rev. B 86, 121403 (2012).
- [4] X. F. Yang, Y.S.Liu, Nanoscale Res. Lett. 5, 1228 (2010).
- [5] Y. Zhang, A. Vishwanath, Phys. Rev. Lett. 105, 206601 (2010).
- [6] Y. X. Li, H. Y. Choi, H. W. Lee, Phys. Lett. A 372, 2073 (2008).
- [7] W. J. Gong, Y. S. Zheng, Y. Liu, F. N. Kariuki, T. Q. Lü, Phys. Lett. A 372, 2934 (2008).
- [8] H. Z. Lu, R. Lu, B. F. Zhu, Phys. Rev. B 71, 235320 (2005).
- [9] Musa Kadhim Shamer, " Electron Transport through a Quantum Dot : Thermoelectric Effects and Correlation Effects in Kondo and Non-Kondo Regimes ", Ph.D. Thesis, Basrah University, Basrah, (2012).



- [10] Hisham Yousif Al- Mhdi," The Chemisorption of Cobalt Atom on Noble Metal Surfaces: Kondo Effect ", M.Sc. Thesis, Basrah University, Basrah, (2008).
- [11] Reman Jamal Jasm," Theoretical Study in the Thermospin Effects for the Quantum Dot in a Magnetic Field ", M.Sc. Thesis, Basrah University, Basrah, (2017).
- [12] Z. C. Yang, Q. F. Sun, X. C. Xie, J. Phys. Condens. Matter 26, 045302 (2014).
- [13] R. N. Shang, H. O. Li, G. Cao, M. Xiao, T. Tu, H. W. Jiang, G. C. Guo, G. P. Guo, Appl. Phys. Lett. 103, 162109 (2013).
- [14] X. T. An, H. Y. Mu, Y. X. Li, J. J. Liu, Phys. Lett. A 375, 4078 (2011).
- [15] Yi. Guangyu, An . Limin , G. WeiJiang , Wu. Haina, C. Xiaohui, Phys. Lett. A 377, 1127–1133 (2013).
- [16] W. Gong, Y. Zheng, Y. Liu, T. Lu, Physica E 40, 618 (2008).
- [17] R. Lopez, R. Aguado, G. Platero, Phys. Rev. Lett. 89, 136802 (2002).
- [18] Z.-Y. Zhang, J. Phys.: Condens. Matt. 17, 1617 (2005).
- [19] M. Lee, Mahn-Soo Choi, R. Lopez, R. Aguado, J. Martinek, R. Zitko, Phys. Rev. B 81, 121311(2010).
- [20] Y. Tanaka, N. Kawakami, A. Oguri, Phys. Rev. B 85, 155314 (2012).
- [21] J. Mravlje, A. Ramsak, T. Rejec, Phys. Rev. B 73, 241305 (2006).
- [22] J.C. Chen, A.M. Chang, M.R. Melloch, Phys. Rev. Lett. 92, 176801 (2004).
- [23] T. S. Kim, S. Hershfield, Phys. Rev. B 63, 245326 (2001).
- [24] P. S. Cornaglia, D. R. Grempel, Phys. Rev. B 71, 075305 (2005).
- [25] R. Taranko, T. Kwapinski, and E. Taranko, Phy. Rev. B 69, 165306 (2004).
- [26] T. Kwapinski and R. Taranko, Eur. Phys. J. B 88: 140 (2015).
- [27] T. Kwapinski, R. Taranko, science direct, Physica E 18, 402 – 411(2003)
- [28] M. Tsukada, Progr. Theor. Phys. 106 (Suppl.) 217(1991).
- [29] R. Taranko, E. Taranko, M. Wiertel, Acta Phys. POL. A 103, 483 (2003).
- [30] M. Wiertel, E. T aranko, R. T aranko, Acta Phys. Pol . A 101, 837 (2002).
- [31] T.B. Grimley , V .C. J yothi Bhasu, K .L. Sebastian, Surf . Sc i. 305 (1983).
- [32] M. Tsukada, Prog Theor Phys. 106 (Suppl) 257(1991).
- [33] R. Taranko,T.Kwapinski, E.Taranko,Phys.Rev.B69, 165306 (2004).
- [34] Thikra S. Dh. Al-Naser," Charge Exchange Process in the Scattering of Irons off Adsorbate – covered Surface ", M.Sc. Thesis, Basrah University, Basrah, (2003).
- [35] Jenan M. Al- Mukh, " charge Transfer Between Atom (Ion) and Metal Surfaces ", Ph.D. Thesis, Basrah University, Basrah, (1997).
- [36] A. S. Davydov, "Quantum Mechanics" Second Russain Edition Published by Nauka, Moscow, (1973).
- [37] Qasim S.K. Al-Shook," Effect of an Absorbed Atom on Resonant Charge Exchange in Atom scattering off solid Surface", M.Sc. Thesis, Basrah University, Basrah, (2010).
- [38] T. Kwapinski, R. Taranko, E. Taranko, Phys. Rev. B 66, 035315 (2002).
- [39] Sun. Qingfend, Lin. Tsunghan, J. Phys. Condens. Matt. 9, 4875 (1997); R. Lopez, R. Aguado, G. Platero, and C. Tejedor, Photonics Spectra 6, 379 (2000).
- [40] T. Mii, K. Makoshi, H. Ueba, Surf. Sci. 493, 575-584 (2001).



- [41] H. M. Obeed." Time-dependent Electron Transport through a Quantum Dot Assisted by Electromagnetic Field: In the Presence and Absence of the Nonresonant Channal", ", M.Sc. Thesis, Basrah University, Basrah, (2014).
- [42] H. Akinaga, T. Manago, M. Shirai, J. Appl. Phys. 2,39 , 1118 (2000).
- [43] V. H. Etgens, P. C. de Camargo, M. Eddrief, R. Mattana, J. M. George, and Y. Garreau, Phys. Rev. Lett. 92, 167205 (2004).
- [44] J. H. Zhao, F. Matsukura, K. Takamura, E. Abe, D. Chiba, and H. Ohno, Appl. Phys. Lett. 79, 2776 (2001).
- [45] J. J. Deng, J. H. Zhao, J. F. Bi, Z. C. Niu, F. H. Yang, X. G. Wu, and H. Z. Zheng, J. Appl. Phys. 99, 093902 (2006).
- [46] K. Ozdogan, E. Sasioglu, and I. Galanakis, J. Magn. Magn. Mater. 322, 46 (2010).
- [47] J. M. Khalaf Al-zyadi," Surface half-metallicity in several binary/ternary compounds", Ph.D. Thesis , Huazhong University of Science and Technology, (2013).
- [48] G. Y. Gao, K. L. Yao, E. Sasioglu, L. M. Sandratskii, Z. L. Liu, J. L. Jiang, Phys. Rev. B 75, 174442 (2007).
- [49] B. G. Liu, Phys. Rev. B 67, 172411 (2003).
- [50] Y. Q. Xu, B.-G. Liu, D. G. Pettifor, Phys. Rev. B 66,184435 (2002).
- [51] W. H. Xie, Y.-Q. Xu, B.-G. Liu, D. G. Pettifor, Phys. Rev. Lett. 91, 037204 (2003).
- [52] W. H. Xie, B.-G. Liu, D. G. Pettifor, Phys. Rev. B 68,134407 (2003).
- [53] B. G. Liu, Lecture Notes in Physics, Vol. 676, pp. 267–291 (Springer, Berlin, (2005)).
- [54] Maged A. Nattiq, Jenan M. Al-Mukh, Jabbar M. Khalaf Al-Zyadi, Journal of Basrah Researches ((Sciences)) Vol. (45). No. 2(2019).